ACS OMEGA

Open Access

http://pubs.acs.org/journal/acsodf

Article

A Biochemical Corrosion Monitoring Sensor with a Silver/Carbon Comb Structure for the Detection of Living *Escherichia coli*

Chiyako Touge, Michiyo Nakatsu, Mai Sugimoto, Eiichiro Takamura, and Hiroaki Sakamoto*

Cite This: *ACS Omega* 2023, 8, 43511−43520

Read Online

ACCESS | Metrics & More | Article Recommendations | Supporting Information

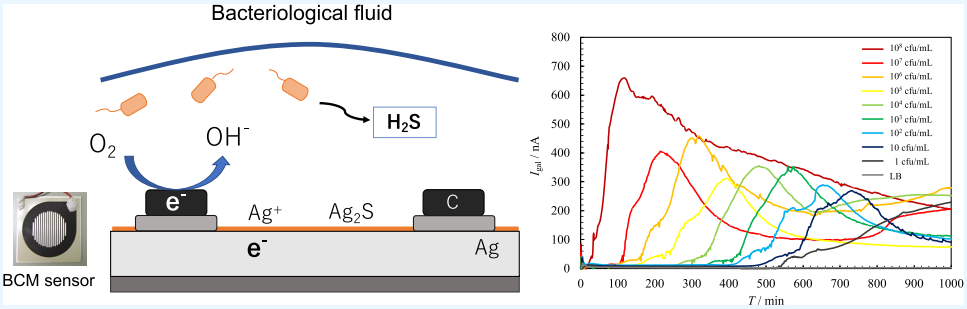

ABSTRACT: For the detection and monitoring of live bacteria, we propose a biochemical corrosion monitoring (BCM) sensor that measures galvanic current by using a Ag/C sensor comprising silver and carbon comb electrodes. The deposition of an *Escherichia coli* suspension containing an LB liquid medium on the Ag/C sensor increased the galvanic current. The time required for the current to reach 20 nA is defined as T_{20}. T_{20} tends to decrease as the initial number of *E. coli* in the *E. coli* solution increases. A linear relationship was obtained between the logarithm of the *E. coli* count and T_{20} in a bacterial count range of $1-10^8$ cfu/mL under culture conditions in which the growth rate of the bacteria was constant. Hence, the number of live *E. coli* could be determined from T_{20}. Ag_2S precipitation was observed on the surface of the Ag electrode of the Ag/C sensor, where an increase in the current was observed. This generation of galvanic current was attributed to the reaction between a small amount of free H_2S metabolized by *E. coli* in the bacterial solution during its growth process and Ag—the sensor anode. The Ag/C sensor can detect a free H_2S concentration of 0.041 μM in the *E. coli* solution. This novel biochemical sensor can monitor the growth behavior of living organisms without damaging them.

INTRODUCTION

Infectious diseases are a serious global health and social problem. A common example of infectious diseases is food poisoning, caused by contamination of food by microorganisms such as *Staphylococcus aureus*, norovirus, and enterohemorrhagic *Escherichia coli*. However, even with technologically advanced medical care, the threat of harmful microorganisms remains significant, as evidenced by the outbreaks of various infectious diseases, such as *E. coli* O157. Therefore, it is particularly important to detect and identify microorganisms for appropriate hygiene management, such as maintaining product safety, preventing biohazards, and identifying the cause of contamination at an early stage in the food and medicinal product industry. Hence, a simple detection method for microorganisms needs to be established.

Some conventional methods for detecting harmful microorganisms include culture methods,[1,2] immunological methods, and genetic engineering methods. The most standardized culture method is inexpensive and allows for the reproductive capacity of the microorganism to be measured by culture. The method also permits a selective culture using a medium in which certain bacteria can grow preferentially. Furthermore, because the number of colonies is counted directly by the naked eye, the culture method does not require special equipment and is therefore very popular in the field. However, rapid detection is not possible with the culture method because the bacteria need to be cultured for approximately 48 h before they can be detected. The immunochromatography method, an immunological technique, has high specificity and simplicity of operation because the detection is based on the antigen−antibody reaction, and it is possible to determine the number of microorganisms within 20 min after a sample is dropped into the kit. However, this method is not suitable for screening tests because, as with the culture method, it requires a long incubation period before each measurement and the antibodies must correspond to the detection target. In addition, this

Received: May 24, 2023
Revised: October 20, 2023
Accepted: October 25, 2023
Published: November 13, 2023

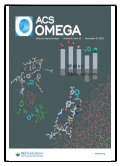

method has a relatively low sensitivity, with a detection limit of 10^4 to10^6 cfu/mL. Some genetic engineering methods such as real-time polymerase chain reaction (PCR)[3,4] and DNA microarrays[5−7] have also been developed for the determination of microorganisms. These methods target microbial DNA for detection. In the real-time PCR method, the target DNA is amplified by PCR and the amplified amount is measured over time using fluorescence to quantify the target DNA. This method has extremely high sensitivity and allows the detection of bacteria at concentrations ≤10 cfu/mL. However, because it uses fluorescence, the equipment is expensive and bulky, making it impractical for use outside of the laboratory. In the DNA microarray detection method, the device comprises a small substrate arrayed with DNA probes complementary to the DNA of many bacteria. In this method, a fluorescently labeled sample is hybridized to the DNA probes on the substrate, and then the presence, or absence, and intensity of fluorescence are measured. However, it is difficult to apply this method to rapid and convenient on-site testing because of the complicated operation that requires labeling of the DNA to be detected and the high cost of detection equipment. Furthermore, immunological and genetic methods quantify the number of microorganisms by utilizing the direct reaction of microorganisms with antibodies or DNA. Therefore, unlike culture methods, they tend to detect dead microorganisms as well.[8]

In general, detection devices for microorganisms should be inexpensive and simple and have low detection limits, high sensitivity, high selectivity, and good reproducibility. Although the aforementioned conventional methods have sufficient sensitivity, they are not very practical because they require long detection times, their measurement devices are costly, and it is difficult to detect live microorganisms using them. Consequently, electrochemical method-based microorganism-detection sensors are attracting increasing attention as an alternate means. Compared to other methods, these sensors afford a rapid response and can detect minute amounts of samples.[9−11] In addition, the detection equipment is inexpensive, compact, and easy to operate.

In this study, we used galvanic currents generated by bimetallic corrosion. When two different metals are immersed in an electrolyte, the metal with the lower potential becomes the anode, and that with the higher potential becomes the cathode, thereby forming a battery. The corrosion caused by the electrochemical reaction between different metals is called galvanic corrosion, and the current generated in this process is called the galvanic current. Microorganism-detection sensors using galvanic current have the advantage of a simple two-electrode configuration, which makes the measurement device more compact and inexpensive than three- or four-electrode sensors. An example of a two-electrode sensor currently in use is the atmospheric corrosion monitoring (ACM) sensor.[12−15] This sensor is widely used to evaluate the metal corrosiveness in atmospheric environments. When the surface of a comb-shaped electrode composed of iron and silver is covered with a thin aqueous film, such as humidity or rain, a galvanic current is generated between the two electrodes owing to the electrolytic mass dissolved in the aqueous film. The currents within the nA to mA range can be measured with good repeatability. Furthermore, the ACM sensor is produced by screen printing, which enables stable quality and mass production. The metal corrosiveness of the atmospheric environment can be evaluated from the electric quantity of the sensor, which is obtained over a monitoring period of approximately a month. Microcurrent measurements of several nanoamers, miniaturization of the ammeter, and monitoring measurements are possible with ACM sensors. However, ACM sensors have not been used for biomeasurements in the medical and food industries.

This study proposes a biochemical corrosion monitoring (BCM) sensor comprising a two-electrode comb-shaped electrode for constructing a simple detection and monitoring system for live microorganisms using galvanic current. *E. coli* is used as the model microorganism to be detected. A Ag/C electrode sensor with silver as the anode and carbon as the cathode is fabricated. A suspension of *E. coli* is dropped onto the electrode surface. We also report the results of a galvanic current response study of live *E. coli* and the investigation of the response mechanism.

EXPERIMENTAL SECTION

Fabrication of the Ag/C Sensor. We fabricated the BCM sensor consisting of a Ag/C galvanic couple, as shown in Figure 1. The Ag/C sensor consists of two electrodes: Ag was

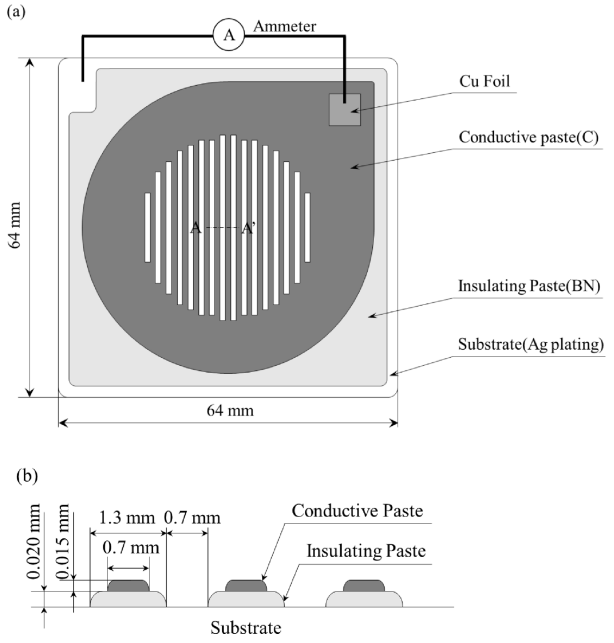

Figure 1. Schematic representation of the sensor. (a) Plane view and (b) enlarged view of the cross section along line A-A′.

on the anode and C on the cathode. The specifications of the Ag/C sensor are shown in Table 1. The insulating layer was a screen-printed epoxy resin (ECCOBOND ME-990J #MBN, Henkel Japan Corp.) on the substrate and thermally cured at 150 °C for 1 h. Next, a carbon resin (Carboloid MRX-713J-A, Tamura Corp.) was laminate-printed on this insulation layer, which was then thermally cured at 130 °C for 30 min. The prototype Ag/C sensor was subjected to the following tests at room temperature (RT, 25 °C), with an insulation resistance of >1 GΩ between the anode and the cathode. The fabricated electrodes were stored in desiccators until immediately before testing.

Preparation of *E. coli* Solution. First, 10 μL of *E. coli* DH5α bacterial solution was dropped onto the plain LB medium, spread using a corn large stick, and incubated at 37

https://doi.org/10.1021/acsomega.3c03632
ACS Omega 2023, 8, 43511−43520

Table 1. Ag/C Sensor Specifications

	substrate area/mm^2	electrode length/mm^2	electrode width/mm^2	anode Ag		cathode C	
				area/mm^2	width/mm	area/mm^2	width/mm
Ag/C	4096	930	0.3	320	0.7	1746[a]	0.7

[a]Wet contact area: 1385 mm^2.

°C overnight. A sterile toothpick was inserted into a single colony on the incubated plate and inoculated into 100 mL of the LB liquid medium in a 500 mL ridged Erlenmeyer flask. The LB liquid medium was prepared by adjusting the composition to 1.0% (w/v) tryptone, 0.5% (w/v) yeast extract, and 0.5% (w/v) NaCl, which was then autoclaved at 121 °C for 15 min and cooled. The pH of the LB liquid medium was 7.0. The *E. coli* solution was transferred to a 50 mL centrifuge tube and centrifuged at 4 °C, 6000 rpm for 10 min. The supernatant was removed, sterile saline was added to it, and the suspension was centrifuged again under the same conditions to remove the supernatant. After the bacteria were washed three times, 20 mL of the LB liquid medium was added to obtain an *E. coli* solution (hereinafter referred to as the "*E. coli* solution"). The *E. coli* concentration was adjusted by measuring the absorbance of the *E. coli* solution at a wavelength of 600 nm using a spectrophotometer (U-3900, HITACHI), where OD_{600} = 1 corresponds to 10^8 cfu/mL and OD_{600} = 0.1 corresponds to 10^7 cfu/mL. A 10^7 cfu/mL *E. coli* solution was diluted stepwise to 10^6 cfu/mL to confirm that there was a linear relationship between the OD value and *E. coli* concentration (Figure S1). The OD_{600} = 0.1 solution was diluted with an LB liquid medium to prepare *E. coli* solutions equivalent to 1−10^7 cfu/mL. Dead *E. coli* solution was sterilized by adding 70 v/v% ethanol to the OD_{600} = 1 solution. The *E. coli* washed under the aforementioned conditions was used to prepare a solution of OD_{600} = 0.1 using 1 mM HEPES buffer (pH 7.0) instead of the LB liquid medium. In this study, the number of *E. coli* at the time of adjustment was used as the initial number of *E. coli*

Galvanic Current Measurement of the Ag/C Sensor Coated with an *E. coli* Solution. Galvanic current response measurements (hereafter termed the "bacterial response test") were performed by dropping the *E. coli* solution onto the Ag/C sensor using the test cell shown in Figure 2a,b. The cell consists of a glass tube (42 mm ID, 32 mm height) fixed to the electrode of the Ag/C sensor to hold the *E. coli* solution. The cell was assembled in an aseptic chamber after autoclaving each part at 121 °C for 15 min and placed in a constant-temperature bath at 37 °C. After 10 mL of the prepared *E. coli* solution was dropped from the upper hole of the test cell, the cell was covered with a silicon culture plug to prevent evaporation of the solution and bacterial contamination from air. The Ag/C sensor was connected to a zero-resistance ammeter (SACM-51FR, Syrinx), and the galvanic current between the electrodes (hereafter referred to as I_{gal}) was measured at 2 min intervals. The test was conducted five times (n = 5) with a new Ag/C sensor for each measurement and the same number of bacteria. In this study, the I_{gal} generated when the Ag electrode of the Ag/C sensor functioned as an anode was expressed as positive. The sensor response threshold was set to 20 nA with a signal-to-noise ratio of 10. The time required for I_{gal} to reach 20 nA was denoted as T_{20}.

Measurement of Corrosion Potential and Galvanic Current of the Ag/C Sensor in the *E. coli* Solution. The Ag electrode potential and I_{gal} of the Ag/C sensor in the *E. coli* solution were measured simultaneously by using a potentio-

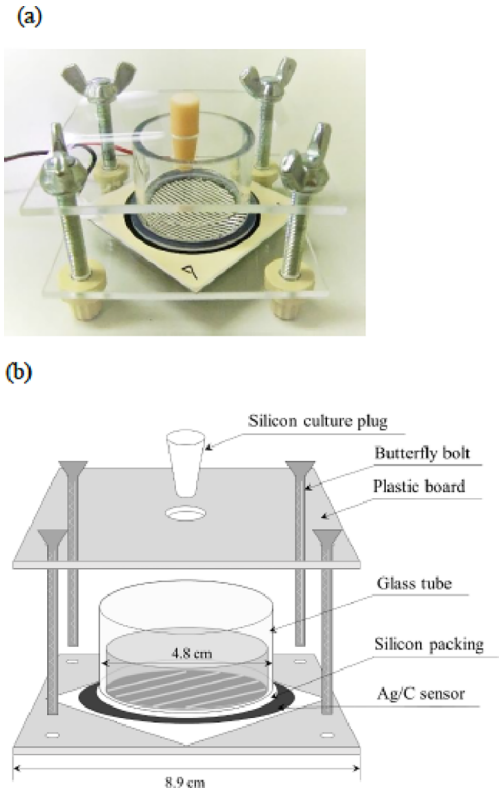

Figure 2. (a) Appearance and (b) schematic representation of the bacterial response test cell.

galvanostat (SI 1287, Solartron) that constitutes a zero-resistance ammeter. The measurements were performed at RT (25 °C) with 20 mL of the *E. coli* solution in the test cell (shown in Figure 2) and a saturated calomel electrode as the reference electrode. Because the cathode potential of the Ag/C sensor is equal to the Ag electrode potential, $E_{[Ag]}$, of the Ag/C sensor, measured $E_{[Ag]}$ was used as the corrosion potential, E_{corr}, of the Ag/C sensor. The potential values in this study were regarded as the standard hydrogen electrode potential (SHE).

Measurement of Cathodic Reduction of Colored Products on the Ag Electrode Surface of the Ag/C Sensor. Electrolytic cathodic reduction[16,17] was used to determine the composition and film thicknesses of colored products on the Ag electrode surface of the Ag/C sensor. A standard three-electrode cell containing deaerated 0.1 M KCl as the electrolyte, a Pt mesh counter electrode, a saturated calomel reference electrode, and the specimen as the working electrode was used. In a 500 mL glass electrolytic cell, 200 mL of the electrolyte was placed. The Ag/C sensors were covered with Teflon tape, except for the electrode part, and the measurement area—the Ag anode—was 320 mm^2, as shown in Table 1. The method employs a constant reducing current to monitor the change in the specimen potential over time during the electrolytic reduction of the colored products. The

https://doi.org/10.1021/acsomega.3c03632
ACS Omega 2023, 8, 43511−43520

reduction was performed at a constant current density of −39 μA/cm^2 using a potentiogalvanostat (SI 1287, Solartron) at RT (25 °C). Electrolysis was terminated when the electrode potential of the specimen reached −1100 mV. The time required for the reduction of the colored products on the Ag electrode, t_{red} (s), was read from the obtained potential−time curve. Using Faraday's law, the average film thickness of a substance being reduced, t (nm), is defined in eq 1as follows:[16,17]

$$t(\mathrm{nm}) = Mit_{red}/(nF\rho) \times 10 \quad (1)$$

where M is the molecular weight (g/mol), i is the electrolytic current density (−39 μA/cm^2), n is the number of electrons required for the reduction reaction, F is the Faraday constant (96,480 C/mol), and ρ is the density (g/cm^3).

Ion Component and Free H_2S Analysis of the *E. coli* Solution with Confirmed Ag/C Sensor Response. The ionic components of the *E. coli* solution in the test cell at the specified time in the bacterial response test were analyzed by ion chromatography (Dionex ICS-3000, Thermo Fisher Scientific K.K., Japan). For cations, the analysis was performed using an IonPac CS 16 column (φ 4 mm × 250 mm), 30 mM of methanesulfonic acid solution as the eluent, and the CSRS-ULTRA II suppressor. For the anion analysis, an IonPac AS 18 (φ 4 mm × 250 mm) column, ASRS-ULTRA II suppressor, and KOH (gradient 15−50 mM) eluent were used. An electrical conductivity detector was used for component analyses of the cations and anions. The *E. coli* solution was centrifuged (4 °C, 1500 rpm, 5 min) before analysis, and the supernatant was used as the analysis sample.

For sulfide ion analysis,[18−20] an ICE AS 1 fast (φ 9 mm × 150 mm) column and ACRS 500 suppressor were used. The eluent was 2 mM H_2SO_4, and the reaction reagent was 0.5 M NaOH. The electrochemical detector was equipped with a Ag electrode and a Ag/AgCl reference electrode. A 31 mM sulfide ion standard solution was prepared by dissolving 0.75 g of $Na_2S{\cdot}9H_2O$ in 100 mL of a degassed 0.1 M NaOH solution. For each experiment, this preserved solution was diluted with 0.1 M NaOH solution to prepare 0.016−1.6 μM of sulfide ion standard solutions, which were used to obtain a linear calibration curve. Next, 25 μL of the *E. coli* solution collected from the test cell was immediately injected into the column for the quantitative analysis of sulfide ions. The quantitation limit of the sulfide ion was experimentally determined to be 0.008 μM from a 10× standard deviation of the blank. In aqueous solution, H_2S exists in the form of H_2S, HS^-, and S^{2-}. Their proportions were determined from the acid dissociation constant and solution pH. In this paper, they are collectively referred to as free H_2S, while the quantified S^{2-} concentration is expressed as the free H_2S concentration.

Polarization Curve Measurement of the Ag/C Sensor Ag and C Electrode Surfaces. Polarization curves of the Ag or C electrode surfaces of the Ag/C sensor in the LB liquid medium or 10^8 cfu/mL *E. coli* solution were measured. A 10^8 cfu/mL *E. coli* solution was incubated at 37 °C for 90 min before measurement. Ion chromatography analysis confirmed that the 10^8 cfu/mL *E. coli* solution at the beginning of the measurement contained more than 0.7 μM free H_2S. A potential dynamic polarization test was performed at a sweep rate of 20 mV/min from a rest potential of 1.0 V for the Ag electrode or from a rest potential of −1.5 V for the C electrode. Electrochemical measurements were performed using a 500 mL glass electrochemical cell, saturated calomel electrode reference electrode, and Pt counter electrode with a potentiogalvanostat (SI 1287, Solartron) at 25 °C in an air atmosphere. Ag/C sensors, which were covered with Teflon tape except for the electrode portion, were used as the test specimens.

RESULTS AND DISCUSSION

Generation of Galvanic Current in the *E. coli* Solutions. Various *E. coli* solutions were dripped onto the Ag/C sensor at 37 °C. Figure 3 shows the variation in I_{gal} of

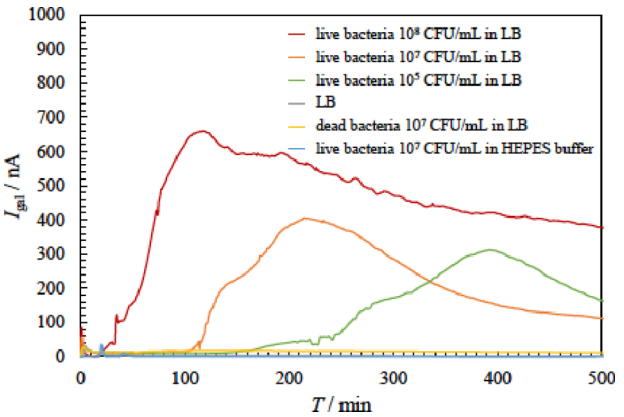

Figure 3. Current changes of the Ag/C sensor when in contact with various *E. coli* solutions at 37 °C.

the Ag/C sensor with each *E. coli* solution in the bacterial response test. Note that 10^8 cfu/mL *E. coli* solution showed a slow increase in I_{gal} at 20 min after the drop was placed on the electrode, reaching a maximum value of 660 nA at approximately 120 min. In the 10^7 cfu/mL *E. coli* solution, I_{gal} started to increase 100 min after the drop was placed on the electrode, and it showed a maximum value of 400 nA at approximately 220 min. In the 10^5 cfu/mL *E. coli* solution, I_{gal} started to increase 140 min after the drop was placed on the electrode. The Ag electrode surface of the Ag/C sensor with elevated I_{gal} showed a brownish coloration after the test instead of the white color of the Ag plating. In contrast, no increase in I_{gal} was observed in the dead *E. coli* solution, the *E. coli* HEPES buffer of 1 × 10^7 cfu/mL, and the LB liquid medium. After the test, there was no coloration on the Ag electrode surfaces of those Ag/C sensors. The Ag/C sensor I_{gal} increased when both live *E. coli* and LB liquid medium were present simultaneously, suggesting a role of *E. coli* growth. We next verified whether the current response obtained in Figure 3 is due to the growth of *E. coli*. Figure 4 shows changes in I_{gal} and OD_{600} of the *E. coli* solution in the test cell during the bacterial response test with a 10^5 cfu/mL *E. coli* solution. OD_{600} of the *E. coli* solution increased rapidly after an induction period of 60 min from the beginning of the test, and then, the rate of increase decreased around 240 min and gradually increased. Based on the change in OD_{600}, the growth rate of *E. coli* can be considered logarithmic from 60 to 240 min and stationary after 400 min. I_{gal} was <10 nA until 140 min after the start of the test and started to increase at approximately 160 min, reaching a maximum at 390 min and subsequently decreasing. I_{gal} began to increase approximately 100 min after OD_{600} started to increase. Thus, I_{gal} began to increase during the logarithmic growth phase of *E. coli* and reached a maximum during the deceleration phase before transitioning to the stationary phase.

https://doi.org/10.1021/acsomega.3c03632
ACS Omega 2023, 8, 43511−43520

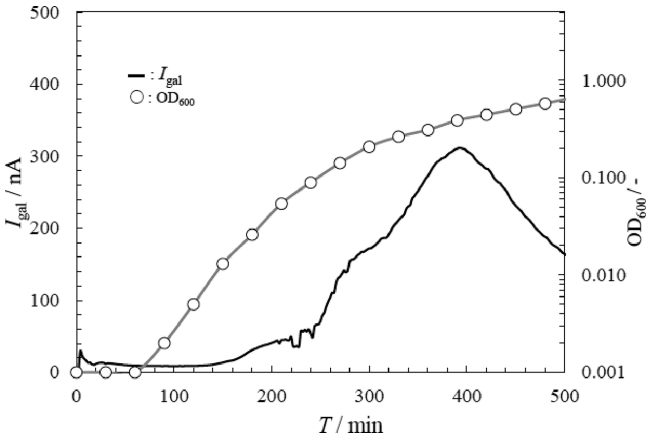

Figure 4. Time variations of the sensor current value and OD_{600} of the test solution in the 10^5 cfu/mL bacterial response test at 37 °C.

As shown in Figure 4, the doubling time (τ) of *E. coli* in the measurement cell during the logarithmic growth phase was 27 min. We confirmed that the doubling time of *E. coli* was also 27 min when the same bacterial solution was incubated at 37 °C without contacting the electrode sensor. Therefore, the *E. coli* in the measurement cell and those incubated without the electrode sensor contact grew at the same rate, indicating no growth inhibition due to contact with the electrode in this study.

Relationship between Current Response and the Initial Number of *E. coli*. Ten levels of *E. coli* solutions were prepared, with an initial bacterial number range of 0−10^8 cfu/mL. We performed a bacterial response test for the Ag/C sensor using the *E. coli* solutions. Figure 5 gives some examples

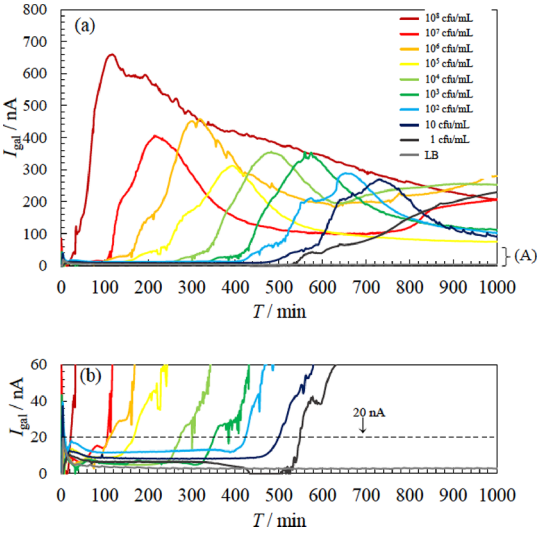

Figure 5. (a) Time variations of the current value of the Ag/C sensor in the bacterial response test using various numbers of *E. coli* at 37 °C. (b) Enlarged view of the (A) range of I_{gal} shown in panel (a).

of the current changes of the Ag/C sensor for each number of *E. coli*. For all solutions with the initial number of *E. coli* in the range of 0−10^8 cfu/mL, the I_{gal} value of the Ag/C sensor remained below 10 nA for a while after the *E. coli* solution was dropped; however, it slowly increased after a predetermined period of time, increasing to the maximum value and then gradually decreasing. It was confirmed that the greater the initial number of *E. coli*, the earlier I_{gal} would increase. *E. coli* solutions with 10^7 cfu/mL or less had a maximum current value of approximately 400 nA, while those of 10^8 cfu/mL had a maximum current value of approximately 600 nA, higher than those of the *E. coli* solutions with 10^7 cfu/mL or less. After the test, the Ag electrode surface of the Ag/C sensor, which exhibited an increase in I_{gal}, was colored brown, as described in the previous section. The intensity of this coloration decreased as the initial number of *E. coli* decreased (Figure S2). It was speculated that the amount of colored products on the Ag electrode decreased as the initial number of *E. coli* decreased.

Figure 6 shows the relationship between the T_{20} obtained from the current curve in the bacterial response test and the

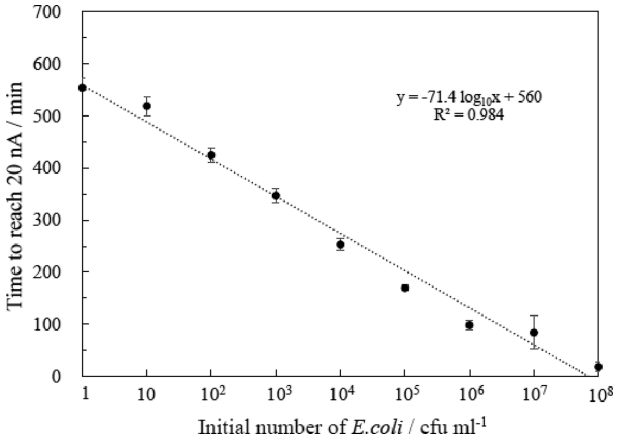

Figure 6. Correlation between the time required for the current value to reach 20 nA in the Ag/C sensor (n = 5) and the initial number of *E. coli* in the bacterial response test.

logarithm of the initial number of *E. coli*, with the mean value of T_{20} in the current curve (n = 5), μ as a symbol, and $\mu \pm \sigma$ (σ: standard deviation) as the upper and lower ends of the error bars. The coefficient of variation is <20% when the initial *E. coli* numbers are 10^7 cfu/mL and <10% otherwise, confirming a high reproducibility in the sensor measurement. When the initial number of *E. coli* is within 1−10^8 cfu/mL, T_{20} tended to decrease with an increasing initial number of *E. coli*. A high correlation was observed between the logarithm of the initial number of *E. coli* (cfu/mL) and T_{20} (min). Subsequently, the linear relationship (R^2 = 0.984) of eq 2 was obtained, where X was the initial number of *E. coli*.

$$T_{20}(\text{min}) = -71.4\log X(\text{cfu/mL}) + 560 (R^2 = 0.984) \quad (2)$$

The T_{20} of 1 cfu/mL for the *E. coli* solution was 560 min. The items that showed a high correlation with the initial number of *E. coli* in the current curve were the time to reach 100 nA (R^2 = 0.997), the time to reach the maximum current value (R^2 = 0.985), the maximum current value (R^2 = 0.572), and the electric quantity for 1000 min (R^2 = 0.776). Therefore, eq 2can be used as a calibration curve for determining the number of live *E. coli* from T_{20}. Furthermore, 1 cfu of live *E. coli* was determined within 560 min.

Corrosion Potential Change and Galvanic Current Generation of the Ag/C Sensor. Figure 7 shows the time variations of E_{corr} and I_{gal} of the Ag/C sensor in a 10^8 cfu/mL *E. coli* solution. E_{corr} decreased from 230 mV immediately after the start of the measurement to −190 mV after 30 min, and I_{gal}

https://doi.org/10.1021/acsomega.3c03632
ACS Omega 2023, 8, 43511−43520

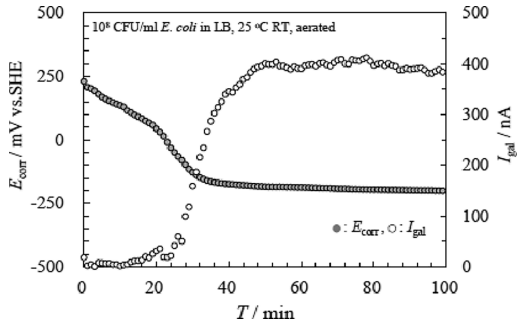

Figure 7. Time variation of E_{corr} and I_{gal} for the Ag/C sensor in a 10^8 cfu/mL *E. coli* solution.

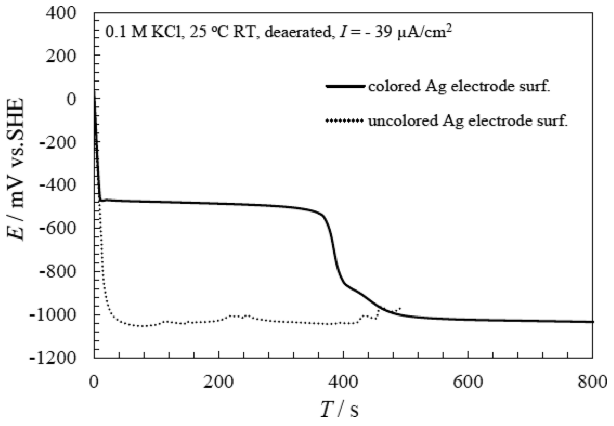

Figure 8. Cathodic reduction curves for the colored and uncolored Ag electrode surfaces of the Ag/C sensor. The colored Ag/C sensor was used in the bacterial response test for the *E. coli* solution with 10^8 cfu/mL, while the uncolored Ag/C sensor was not.

was generated simultaneously. At a potential of approximately 230 mV, which corresponds to the initial E_{corr} of the *E. coli* solution at approximately pH 7, the stable phase is the Ag metal, as shown in the Qpotential-pH equilibrium diagram for the Ag−S−Cl−CO_2−H_2O system at 25 °C.[21,22] However, at an E_{corr} of −190 mV observed after 30 min, the stable phase was Ag_2S. It can be suggested that Ag undergoes the sulfidation reaction on the anode surface of the Ag/C sensor, which results in the generation of I_{gal}.

Colored Products on the Ag Electrode Surface of Ag/C Sensors. The Ag/C sensor that exhibited an increase in I_{gal} during the bacterial response test had a brownish Ag electrode surface, as described in previous sections. The colored area was elementally analyzed using an electron probe microanalyzer (EPMA) (JXA-8530F JEOL Ltd.). On the surface of the Ag electrode of the unused Ag/C sensor, only the Ag elements of the Ag plating layer were detected. In contrast, the $K_{\alpha 1}$ spectrum of the S element was detected at 0.537 nm in addition to the Ag element from the colored Ag electrode surface (Figure S3). X-ray photoelectron spectroscopy (XPS: Mg−K_α X-ray, JPS-9010MCY JEOL Ltd.) was used to characterize the brownish Ag electrode surface of the Ag/C sensor after the bacterial response test. The peak values in the S $2p_{3/2}$, Ag $3d_{2/5}$, and O 1s profiles at the Ag electrode surface are shown in Table S1 as the binding energies. The binding energies were calibrated against the binding energy of the C 1s electron (285.0 eV) as a reference. The binding energy of S $2p_{3/2}$ shifts from 164 eV corresponds to S^0 to 162.7 eV on the low energy side, suggesting the possibility of Ag sulfide formation.[23] The precipitates deposited on the colored Ag electrode surface were scraped off and recovered. Structural analysis of that recovered powder was performed by an X-ray diffraction pattern (XRD: CuK_α, 40 kV, 100 mA, RINT TTR2FK Rigaku Corp.). In the X-ray diffraction pattern of the precipitates, Ag_2S peaks at 34.385 and 36.805°[24] were slightly observed (Figure S4).

Figure 8 shows cathodic reduction curves for the colored and uncolored Ag electrode surfaces of the Ag/C sensor obtained from the cathodic stripping experiment. The electrode potential of the colored Ag electrode surface decreased from an E_{corr} of 40 mV, became constant at approximately −530 mV for t_{red} = 380 s, and then decreased sharply again. The disappearance of coloration on the electrode surface was visually confirmed at the Ag metal electrode potential of approximately −756 mV. The plateau potential of −530 mV, as shown in the curve, was attributed to the reduction of the Ag_2S film.[16] The amount of Ag_2S deposited on the Ag electrode surface was calculated to be 246 nmol from t_{red}. The average thickness of that film, t, was calculated to be 26 nm from eq 1, where M = 247.8 g/mol, ρ = 7.32 g/cm^3, and n = 2 (because Ag_2S is reduced to Ag metal). The colored sensor was prepared by galvanic corrosion in a bacterial response test for *E. coli* solution with 10^8 cfu/mL. The integrated electric charge of I_{gal} at that time was 48 mC, and it was calculated that 249 nmol of Ag_2S was deposited on the Ag electrode surface. Therefore, the amount of Ag_2S deposited on the Ag electrode surface was found to be almost the same as the amount of cathodic stripped Ag_2S. The electrode potential of the uncolored Ag electrode surface dropped sharply from E_{corr} of −30 mV and reached approximately −1000 mV after 20 s. No Ag_2S was deposited on the uncolored Ag electrode surface of the Ag/C sensor. The formation of the Ag_2S film on the anode surface supports the occurrence of the sulfidation reaction on the Ag electrode surface, as described in the previous section. The solubility of Ag_2S in an aqueous solution, 6.15×10^{-13} g/L, is remarkably low.[25] Therefore, Ag_2S was presumably expected to precipitate on the Ag electrode surface immediately after its generation in the *E. coli* solution.

Analysis of Sulfur Compounds in *E. coli* Solution during Increasing Galvanic Current. Table 2 shows the ionic composition and pH of the *E. coli* solution in the test cell at 0, 120, and 1200 min in the 10^8 cfu/mL bacterial response test. NO_3^- and NH_4^+ increased at 120 min; however, the concentrations of other ions did not change significantly. A lead−acetate−paper test confirmed the generation of H_2S in the *E. coli* culture in the LB liquid medium.[26] It was also reported that 0.36 μM of H_2S was generated 24 h after the start of *E. coli* culture using TSI broth.[27] Similarly, in the bacterial response test conducted in this study, sulfur compounds, such as H_2S metabolized by *E. coli*, are likely released into the *E. coli* solution during the growth process. It is assumed that these sulfur compounds sulfurize the Ag electrode surface of the Ag/C sensor. *E. coli* has a metabolic pathway in which L-cysteine dehydrogenase catalyzes the degradation of L-cysteine to produce pyruvate, NH_3, and H_2S (eq 3).[28,29]

$$HSCH_2CH(NH_2)COOH + H_2O \rightarrow CH_3COCOOH + H_2S + NH_3 \quad (3)$$

The H_2S produced is transferred outside the bacteria. The H_2S released into living cells, such as the pancreas and brain,

https://doi.org/10.1021/acsomega.3c03632
ACS Omega 2023, 8, 43511−43520

Table 2. Ion Chromatographic Analysis Results of the Test Solution in the 10^8 cfu/mL Bacterial Response Test

test solution		LB liquid medium containing 10^8 cfu/mL *E.coli*			LB liquid medium
T/min[a]		0	120	1200	
I_{gal}/nA[b]		0	660	200	
ion/mM	Na^+	86	87	86	85
	NH_4^+	4.6	8.3	15	3.9
	K^+	9	9	9	10
	Mg^{2+}	0.20	0.20	0.12	0.03
	Ca^{2+}	0.11	0.12	0.052	0.049
	Cl^-	82	81	82	82
	NO_3^-	0.77	2.1	0.00	0.23
	SO_4^{2-}	0.53	0.54	0.43	0.42
pH/-		6.7	5.6	7.9	7.0

[a]Elapsed time after the start of the bacterial response test. [b]Current value of the Ag/C sensor in the bacterial response test.

quickly forms disulfide bonds with the −SH group ends of proteins and amino acids to form bound sulfur. In living tissues, H_2S exists as bound sulfur, acid-labile sulfur, and free H_2S.[30,31] Because the LB liquid medium containing tryptone and amino acids was added to the *E. coli* solution in this study, H_2S metabolized by *E. coli* is presumed to exist as free H_2S, although some of it is bound to amino acids and other substances.

Figure 9a shows the time variations in the I_{gal} of the Ag/C sensor and free H_2S concentration of the test solution in the 10^6 cfu/mL bacterial response test. The chromatograms of the

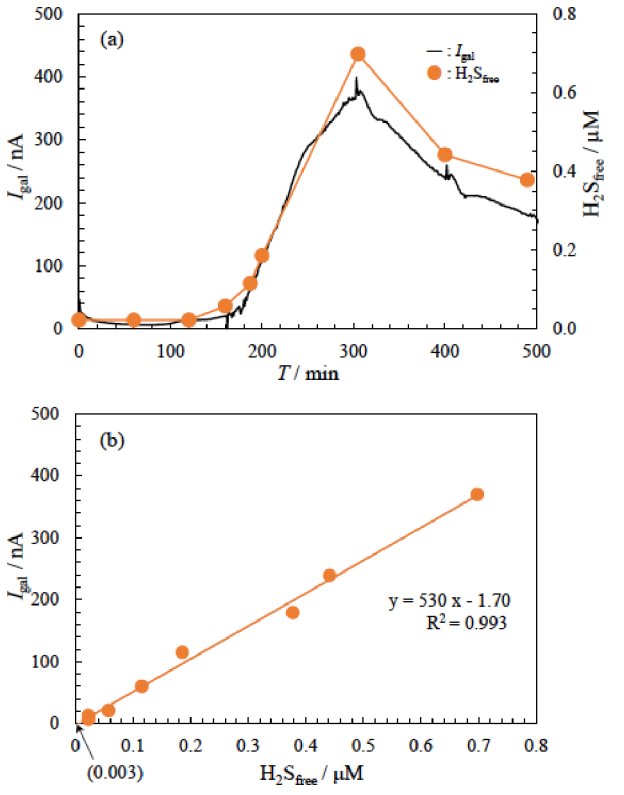

Figure 9. (a) Time variations of the sensor current value and free H_2S concentration of test solution in the 10^6 cfu/mL bacterial response test at 37 °C. (b) Correlation between I_{gal} and free H_2S concentration shown in panel (a).

E. coli solutions are also shown in Figure S5. The concentration of free H_2S in the *E. coli* solution remained approximately 0.022 μM from the start of the test until 120 min; it increased to 0.058 μM when I_{gal} increased to 21 nA at 160 min and then to 0.70 μM when I_{gal} reached 376 nA at 300 min. Thereafter, the free H_2S concentration decreased as the I_{gal} decreased. Figure 9b shows the relationship between the free H_2S concentration and I_{gal} in the *E. coli* solution, revealing a strong linear relationship (R^2 = 0.991) of I_{gal} with the free H_2S concentration. The equation relating I_{gal} to free H_2S is shown in eq 4, where I_{gal} is the galvanic current value of the sensor and $[H_2S_{free}]$ is the concentration of free hydrogen sulfide. The *X*-axis intercept extrapolated from this line would indicate the detection limit of the sensor for free H_2S, which was 0.003 μM. The *E. coli* solution with an I_{gal} of <10 nA from the beginning of the bacterial response test to 120 min has a free H_2S concentration of 0.022 μM. Equation 4 indicates that a free H_2S concentration of ≥0.041 μM is required to increase the sensor current value to ≥20 nA. In Figure 9a, the free H_2S concentration of the *E. coli* solution when I_{gal} reached 21 nA was 0.058 μM, which was above 0.041 μM. The increase in the I_{gal} of the Ag/C sensor is presumably caused by the reaction of the Ag electrode with the increased free H_2S in the *E. coli* solution.

$$I_{gal}(\text{nA}) = 530[H_2S_{free}](\mu\text{M}) - 1.70 \quad (R^2 = 0.993) \tag{4}$$

Electrode Reactions of the Ag/C Sensor in *E. coli* Solution. Figure 10 shows polarization curves of each Ag/C

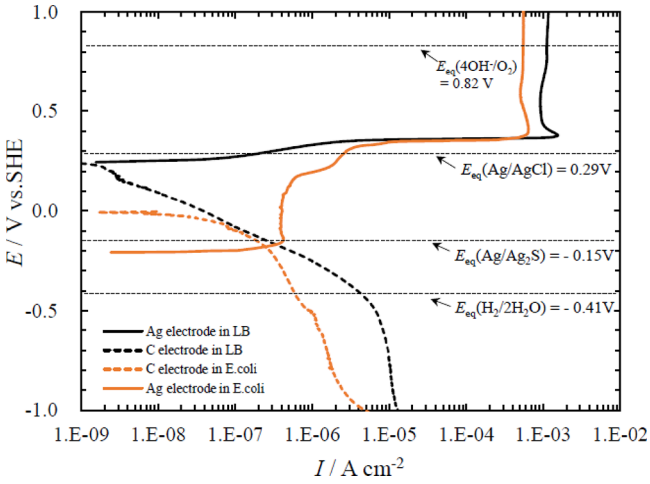

Figure 10. Polarization curves for the Ag or C electrodes of the Ag/C sensor in the LB liquid medium or in 10^8 cfu/mL *E. coli* solution incubated for 90 min at 37 °C.

sensor electrode in the LB liquid medium or 10^8 cfu/mL *E. coli* solution. The anodic current density of the Ag electrode in the LB liquid medium increased rapidly at a rest potential of 0.23 V and then became a constant value above 0.4 V. The cathodic current density of the C electrode in the LB liquid medium gradually increased from a rest potential of 0.23 V, showing a current density of approximately 10 μA/cm^2 below −0.5 V. The increase in the anodic current density at approximately 0.30 V is consistent with the equilibrium potential E_{eq} (Ag/AgCl, 0.085 M Cl^-) = 0.29 V. The main components of precipitates on the surface of the Ag electrode polarized from a rest potential to 1.0 V were detected as Ag and Cl elements by X-ray fluorescence analysis. Accordingly, the Ag/AgCl reaction

https://doi.org/10.1021/acsomega.3c03632
ACS Omega 2023, 8, 43511−43520

(eq 9) was inferred to occur at the surface of the Ag electrode because the LB liquid medium and *E. coli* solution contain 0.085 M NaCl.

The anode current density of the Ag electrode in the *E. coli* solution increased rapidly from a rest potential of −0.21 V and then remained at or above 400 nA/cm^2 in the potential range from −0.17 to approximately 0.17 V. Upon further increasing the potential, the anode current density increased sharply again, as did that of the Ag electrode in the LB liquid medium and reached a constant value above 0.4 V. The rest potential value of −0.21 V shifted 0.44 V lower than the rest potential value of the Ag electrode in the LB liquid medium and was below the equilibrium potential E_{eq}(Ag/Ag$_2$S, pH 7) = −0.15 V.[21−23] These results support the changes in E_{corr} values shown in Figure 7. The cathodic current density of the C electrode in the *E. coli* solution increased gradually from a rest potential of 0 V, showing a current density of approximately 1 μA/cm^2 below −0.5 V. Free H_2S released from *E. coli* exists mainly in H_2S and HS^- forms in *E. coli* solution at a pH of approximately 7 because of the acid dissociation equilibrium of H_2S (eq 5). The main components of precipitates on the surface of the Ag electrode polarized from rest potential to 0.2 V were detected as Ag and S elements by X-ray fluorescence analysis. Therefore, the reaction of HS^- and H_2S in *E. coli* solution with the Ag electrode (eqs 6and 7) was considered to occur on the Ag electrode surface.

$$H_2S_{free} \rightarrow HS^- + 2H^+ pK_{a1} = 7.02 \quad (5)$$

$$2Ag + H_2S \rightarrow Ag_2S + 2H^+ + 2e^- \quad (6)$$

$$2Ag + HS^- \rightarrow Ag_2S + H^+ + 2e^- \quad (7)$$

$$2Ag + S^{2-} \rightarrow Ag_2S + 2e^- \quad (8)$$

$$Ag + Cl^- \rightarrow AgCl + e^- \quad (9)$$

The main cathodic currents in aqueous solution under atmospheric conditions are the reduction reaction of dissolved oxygen (eqs 10and 11) and the reduction reaction of H^+ (eqs 12 and 13). In aqueous solution at a pH of approximately 7, the reactions of eqs 11 and 13 are predominant, and their equilibrium potentials are E_{eq} ($4OH^-/O_2$, pH 7) = 0.82 V and E_{eq} ($H_2/2H_2O$, pH 7) = −0.41 V, respectively. Therefore, the cathodic current of the C electrode shown in Figure 10 was estimated to be the reduction current of dissolved oxygen (eq 11) in the potential range from the rest potential to approximately −0.41 V, and the reduction current of H^+ (eq 13) was added below −0.41 V.

$$O_2 + 4H^+ + 4e^- \rightarrow 2H_2O \quad (10)$$

$$O_2 + 2H_2O + 4e^- \rightarrow 4OH^- \quad (11)$$

$$2H^+ + 2e^- \rightarrow H_2 \quad (12)$$

$$2H_2O + 2e^- \rightarrow H_2 + 2OH^- \quad (13)$$

Since the polarization test was conducted under atmospheric pressure, the test solution was supplied with sufficient oxygen. However, the cathodic current density of the C electrode in *E. coli* solution was lower than that of the C electrode in the LB liquid medium in the potential range from 0 to −1.0 V. This was assumed to be due to the decreased dissolved oxygen in the *E. coli* solution caused by the bacterial growth activity. In *E. coli* solution containing H_2S and HS^-, the anodic current clearly increases due to the occurrence of the Ag/AgS reaction (eqs 6and 7). The increase in I_{gal} of the Ag/C sensor in the *E. coli* solution was attributed to the increase in the anodic current density of the Ag electrode due to the reaction of the Ag electrode with H_2S metabolized by *E. coli*. Therefore, the reaction mechanism of the electrode is as follows: The oxidation reactions shown in eqs 6and 7 occur on the anode surface of the Ag/C sensors. On the cathode surface, the reduction reaction (eq 11) involving dissolved oxygen occurs in the *E. coli* solution with a pH of approximately 7, generating a galvanic current between the electrodes.

When the maximum I_{gal} value of 376 nA shown in Figure 9a flows through the Ag/C sensor for 120 s, the total electrical quantity of the sensor becomes 46 μC. If the electric quantity of 46 μC is the current generated by the reaction in eq 6, then, based on Faraday's law, 0.23 nmol of H_2S, corresponding to 0.023 μM in 10 mL of *E. coli* solution, will react with the Ag electrode to generate 0.23 nmol of Ag_2S. Figure 9 shows that the *E. coli* solution has 0.70 μM free H_2S at 376 nA. It was thought that approximately 3.3% of free H_2S present in the *E. coli* solution reacted with the Ag electrode, generating a galvanic current. The Ag/C sensor reacts with the free H_2S increased by the growth of *E. coli*, and I_{gal} rises. T_{20} was estimated to be the time required for the free H_2S concentration in the *E. coli* solution to exceed the detection limit of the Ag/C sensor. Under culture conditions in which the amount of free H_2S metabolized per unit of *E. coli* is equal, the higher the initial number of *E. coli*, the faster the rate of increase in the free H_2S concentration in the *E. coli* solution, and thus the shorter the T_{20}. Therefore, a linear relationship between the logarithm of the initial number of *E. coli* and T_{20} was established, as shown in eq 2.

CONCLUSIONS

A prototype Ag/C sensor comprising a two-electrode comb-shaped electrode was fabricated for constructing a simple detection and monitoring system for detecting live bacteria using a galvanic current. The *E. coli* solution was dropped on the electrode surfaces, and the response of galvanic current to *E. coli* and the response mechanism were investigated. The Ag/C sensor showed an increase in the galvanic current in the *E. coli* solution containing the LB liquid medium. The time required for the current to reach 20 nA is defined as T_{20}. T_{20} tends to decrease as the initial number of *E. coli* in the *E. coli* solution increases. A linear relationship is obtained between the logarithm of the initial number of *E. coli* from 1 to 10^8 cfu/mL and T_{20} under culture conditions where the growth rates of *E. coli* are equal. Hence, the number of live *E. coli* cells can be determined from T_{20}. With increasing current, Ag_2S precipitation was observed on the surface of the Ag electrode of the Ag/C sensor, perhaps owing to the reaction of Ag in the anode with a small amount of free H_2S metabolized by *E. coli* in the *E. coli* solution during the growth process. The Ag/C sensor can detect a free H_2S concentration of 0.041 μM in the *E. coli* solution. The current response of the two-electrode comb-shaped electrode was successfully used to determine the counts of live *E. coli* in a bacterial number range of 1−10^8 cfu/mL. This sensor is novel in that it detects the number of viable bacteria by growing them in the same manner as that in the culture method without using a mediator. The sensor is expected to be applied for the trace hydrogen sulfide analysis of water, food, blood, and biological tissues.

https://doi.org/10.1021/acsomega.3c03632
ACS Omega 2023, 8, 43511−43520

■ ASSOCIATED CONTENT

Supporting Information

The Supporting Information is available free of charge at https://pubs.acs.org/doi/10.1021/acsomega.3c03632.

Figure S1: Correlation between the logarithm of *E. coli* and logarithm of OD_{600}. Figure S2: Photographs of the Ag/C sensor surface after the bacterial response tests. Figure S3: Results of elemental analysis of the colored Ag electrode surface of the Ag/C sensor with an electron probe microanalyzer (JXA-8530F JEOL Ltd.). Figure S4: X-ray diffraction pattern of precipitates deposited on the colored Ag electrode surface of the Ag/C sensor and its enlarged view (Ag_2S: 2θ= 31.520, 36.805, and 37.718°). Figure S5: Ion chromatography analysis results of each test solution at 0, 160, and 187 min in the 10^6 cfu/mL bacterial response test shown in Figure 9a. Table S1: Binding energy values of C 1s, S $2p_{3/2}$, Ag $3d_{5/2}$, and O 1s spectra for the colored Ag electrode surface of Ag/C by XPS measurement (XPS: Mg−Kα X-ray, JPS-9010MCY JEOL Ltd.) (PDF)

■ AUTHOR INFORMATION

Corresponding Author

Hiroaki Sakamoto − *Department of Frontier Fiber and Technology and Science, Graduate School of Engineering, University of Fukui, Fukui 910-8507, Japan;* orcid.org/0000-0002-6300-4055; Phone: +81 776279753; Email: hisaka@u-fukui.ac.jp; Fax: +81 776278747

Authors

Chiyako Touge − *Industrial Technology Center of Fukui Prefecture, Fukui 910-0102, Japan*

Michiyo Nakatsu − *Industrial Technology Center of Fukui Prefecture, Fukui 910-0102, Japan*

Mai Sugimoto − *Department of Frontier Fiber and Technology and Science, Graduate School of Engineering, University of Fukui, Fukui 910-8507, Japan*

Eiichiro Takamura − *Department of Frontier Fiber and Technology and Science, Graduate School of Engineering, University of Fukui, Fukui 910-8507, Japan*

Complete contact information is available at: https://pubs.acs.org/10.1021/acsomega.3c03632

Author Contributions

This manuscript was written through contributions of all of the authors. All authors have approved the final version of the manuscript.

Notes

The authors declare no competing financial interest.

■ REFERENCES

(1) Bessède, E.; Delcamp, A.; Sifrè, E.; Buissonnière, A.; Mègraud, F. New methods for detection of campylobacters in stool samples in comparison to culture. *J. Clin. Microbiol.* **2011**, *49*, 941−944.

(2) Conza, L.; Casati, S.; Gaia, V. Detection limits of Legionella pneumophila in environmental samples after co-culture with Acanthamoeba polyphaga. *BMC. Microbiol.* **2013**, *13*, 49−54.

(3) Schabereiter-Gurtner, C.; Selitsch, B.; Rotter, M. L.; Hirschl, A. M.; Willinger, B. Development of novel real-time PCR assays for detection and differentiation of eleven medically important *Aspergillus* and *Candida* species in clinical specimens. *J. Clin. Microbiol.* **2007**, *45*, 906−914.

(4) Lee, Y. D.; Shannon, K.; Beaudette, A. L. Detection of bacterial pathogens in municipal wastewater using an oligonucleotide microarray and real-time quantitative PCR. *J. Microbiol. Methods* **2006**, *65*, 453−467.

(5) Zhou, G.; Cao, B.; Dou, Y.; Liu, Y.; Feng, L.; Wang, L. PCR methods for the rapid detection and identification of four pathogenic Legionella spp. and two Legionella pneumophila subspecies based on the gene amplification of gyrB. *Appl. Microbiol. Biotechnol.* **2011**, *91*, 777−787.

(6) Petersenl, J.; Poulsen, L.; Petronis, S.; Birgens, H.; Dufva, M. Use of a multi-thermal washer for DNA microarrays simplifies probe design and gives robust genotyping assays. *Nucleic Acids Res.* **2008**, *36*, e10.

(7) Jones, J.; Powell, G. N.; Tristram, A.; Fiander, N. A.; Hibbitts, S. Comparison of the Papillocheck DNA micro-array human papillomavirus detection assay with hybrid capture II and PCR-enzyme immunoassay using the GP5/6+ primer set®. *Journal of Clinical Virology* **2009**, *45*, 100−104.

(8) Karbelkar, A. A.; Furst, L. A. Electrochemical diagnostics for bacterial infectious diseases. *ACS Infectious Diseases* **2020**, *6*, 1567−1571.

(9) Mohankumar, P.; Ajayan, J.; Mohanraj, T.; Yasodharan, R. Recent developments in biosensors for healthcare and biomedical application: A review. *Measurement* **2021**, *167*, 108293.

(10) Rochelet, M.; Solanas, S.; Betelli, L.; Chantemesse, B.; Vienney, F.; Hartmann, A. Rapid amperometric detection of Escherichia coli in wastewater by measuring β-D glucuronidase activity with disposable carbon sensors. *Anal. Chim. Acta* **2015**, *892*, 160−166.

(11) Mann, T. S.; Mikkelsen, S. R. Antibiotic susceptibility testing at a screen-printed carbon electrode array. *Anal. Chem.* **2008**, *80* (3), 843−848.

(12) Xia, D.; Deng, C.; Macdonald, D.; Jamali, S.; Mills, D.; Luo, J.; Strebl, G. M.; Amiri, M.; Jin, M.; Song, S.; Hu, W. Electrochemical measurements used for assessment of corrosion and protection of metallic materials in the field: A critical review. *Journal of Material Science and Technology* **2022**, *112*, 151−183.

(13) Motoda, S. i.; Suzuki, Y.; Shinohara, T.; Kojima, Y.; Tsujikawa, S.; Oshikawa, W.; Itomura, S.; Fukushima, T.; Izumo, S. ACM (Atmospheric Corrosion Monitor) type corrosion sensor to evaluate corrosivity of marine atmosphere. *Corros. Eng.* **1994**, *43*, 550−556.

(14) Oshikawa, W.; Itomura, S.; Shinohara, T.; Tsujikawa, S. ACM Sensor Output to Estimate Atmospheric Corrosion Rate of Carbon Steel Exposed under Conditions Sheltered from Rain. *Corros. Eng.* **2002**, *51*, 398−403.

(15) Nakatsu, M.; Sasahara, K. Evaluation of atmospheric corrosion behaviors of carbon steel and corrosive environmental factors in Fukui. *Corrosion Engineering* **2013**, *62*, 426−429.

(16) Minamitani, R.; Onuki, A.; Matsui, T. Estimation of corrosion thickness of silver concerning seasonal variation of temperature and relative humidity. *Corros. Eng.* **2009**, *58*, 158−163.

(17) Wolfenden, A.; Krumbein, S. J.; Newell, B.; Pascucci, V. Monitoring environmental tests by coulometric reduction of metallic control samples. *J. Test. Eval.* **1989**, *17*, 357−367.

(18) Bond, M. A.; Heritage, D. I.; Wallace, G. G.; McCormick, J. M. Simultaneous determination of free sulfide and cyanide by ion chromatography with electrochemical detection. *Anal. Chem.* **1982**, *54*, 582−585.

(19) Takata, T.; Jung, M.; Matsunaga, T.; Ida, T.; Morita, M.; Motohashi, H.; Shen, X.; Kevil, G. C.; Fukuto, M. J.; Akaike, T. Methods in sulfide and persulfide research. *Nitric Oxide* **2021**, *116*, 47−64.

(20) Dekker, S.; Nardin, T.; Fedrizzi, B.; van Leeuwen, A. K.; Larcher, R. Monitoring hydrogen sulfide de-novo formation from polysulfides present in wine using ion chromatography and ultra high-pressure liquid chromatography combined with fraction collection and high-resolution mass spectrometry. *Journal of Chromatography A* **2023**, *1690*, 463805.

(21) Graedel, E. T. Corrosion mechanisms for silver exposed to the atmosphere. *J. Electrochem. Sci.* **1992**, *139*, 1963−1970.

(22) Szekely, S. T.; Schmitt, H. H. *Equilibrium diagrams for minerals at low temperature and pressure*; Geological Club of Harvard: Cambridge, 1962.
(23) Moulder, J. F.; Stickle, W. F.; Sobol, P. E.; Bomben, K. D. *Handbook of X-ray Photoelectron Spectroscopy*; Physical Electronics Inc., Eden Prairie: Minnesota, U. S. A., 1995.
(24) *Powder Diffraction File*; Joint Committee on Powder Diffraction Standards: Philadelphia, 1972.
(25) Peiffer, S.; Frevert, T. Potentiometric determination of heavy metal sulphide solubilities using a pH_2S (glass|Ag°, Ag_2S) electrode cell. *Analyst* **1987**, *112* (7), 951−954.
(26) Tanaka, N.; Hatano, T.; Saito, S.; Wakabayashi, Y.; Abe, T.; Kawano, Y.; Ohtsu, I. Generation of hydrogen sulfide from sulfur assimilation in Escherichia coli. *J. Gen. Appl. Microbiol.* **2019**, *65*, 234−239.
(27) Thompson, R.; Perry, D. J.; Stanforth, P. S.; Dean, R. J. Rapid detection of hydrogen sulfide produced by pathogenic bacteria in focused growth media using SHS-MCC-GC-IMS. *Microchemical Journal* **2018**, *140*, 232−240.
(28) Awano, N.; Wada, M.; Mori, H.; Nakamori, S.; Takagi, H. Identification and functional analysis of *Escherichia coli* cysteine desulfhydrases. *Appl. Environ. Microbiol.* **2005**, *71* (7), 4149−4152.
(29) Guarneros, G.; Ortega, M. Cysteine desulfhydrase activities of Salmonella typhimurium and *Escherichia coli*. *Biochemi. Biophys. Acta.* **1970**, *198*, 132−142.
(30) Ishigami, M.; Hiraki, K.; Umemura, K.; Ogasawara, Y.; Ishii, K.; Kimura, H. A source of hydrogen sulfide and a mechanism of its release in the brain. *Antioxidants and Redox Signaling* **2009**, *11*, 205−214.
(31) Kimura, Y.; Koike, S.; Shibuya, N.; Lefer, D.; Ogasawara, Y.; Kimura, H. 3-Mercaptopyruvate sulfurtransferase produces potential redox regulators cysteine and glutathione-persulfide (Cys-SSH and GSSH) together with signaling molecules H_2S_2, H_2S_3 and H_2S. *Sci. Rep.* **2017**, *7*, 10459.

https://doi.org/10.1021/acsomega.3c03632
ACS Omega 2023, 8, 43511−43520